THE ASTROPHYSICAL JOURNAL, 332:940–953, 1988 September 15

SYMMETRY OF THE RADIO EMISSION FROM TWO HIGH-LATITUDE SUPERNOVA REMNANTS, G296.5+10.0 AND G327.6+14.6 (SN 1006)

R. S. ROGER[1]
Dominion Radio Astrophysical Observatory, Herzberg Institute of Astrophysics, National Research Council of Canada

AND

D. K. MILNE, M. J. KESTEVEN, K. J. WELLINGTON, AND R. F. HAYNES
Division of Radiophysics, CSIRO, Australia
Received 1987 July 20; accepted 1988 March 17

ABSTRACT

We present new high-resolution radio observations at 843 MHz of the shell supernova remnants G296.5+10.0 and G327.6+14.6. The remnants show a high degree of bilateral symmetry, both in their emission intensities and in the outer boundaries of the emission. Both remnants show weak emission and indistinct boundaries near the axes of symmetry. We explore various explanations of the symmetry, which is apparent in both the radio and X-ray maps, and extend an old idea that it is the result of the expansion of a remnant into a region with an orderly alignment of the ambient interstellar magnetic field oriented with a substantial component normal to the line of sight. The observations are consistent with a scenario in which the production of the emitting particles is more effective in shocks propagating transverse to the field lines. This explanation rests upon the fact that measurements of collisionless shocks in the Earth's magnetosphere and in interplanetary space show significant differences between the structures of quasi-parallel and quasi-perpendicular shocks and upon the recent work of Jokipii which shows that the relativistic particle acceleration rate will be a strong function of the angle between the shock normal and the field direction. G296.5+10.0, the more evolved of the two remnants shows a distinctly larger diameter along the symmetry axis than across it. This suggests that under certain conditions, the coupling of the kinetic energy of the shocked material to newly swept-up gas may be incomplete for shocks propagating approximately along field lines. These various effects may also be present in low-latitude remnants but may not be easily discerned because of more disorderly magnetic field in the Galactic plane.

On the large scale the X-ray and radio emission show similar distributions in each remnant, but with no detailed correspondence of features. The radio emission from G296.5+10.0 shows some fine structure in the form of filaments aligned tangentially to the shell. We interpret the filaments as multiple sheets or crushed clouds seen on edge, partially compressed and cooled yet still too hot to radiate substantially in the visible.

Subject headings: nebulae: supernova remnants — radio sources: extended — shock waves

I. INTRODUCTION

Radio maps of extended supernova remnants provide us with two-dimensional projected views of the interaction of expanding shells of gas with the ambient interstellar medium. Although we have a general understanding that the coupling of the kinetic energy of the supernova ejecta to the interstellar gas is through the turbulent mixing behind collisionless shocks, the details of the interaction are not well understood. Statistical studies of the average radio brightness of SNRs of various sizes (e.g., Milne 1979; Caswell and Lerche 1979) show marked scatter about the mean. Although some of this variation can be attributed to uncertainties in the distances to various remnants (and hence their physical sizes), similar studies of the SNRs in the Large Magellanic Cloud, which are essentially all at the same distance (Mills *et al.* 1984), also show considerable variation in brightness. Variations in brightness are also readily apparent within single remnants. Extended SNRs in the Galactic plane are often irregular in form, a fact usually attributed to nonuniformities in the density of the interstellar medium.

In spite of brightness variations from remnant to remnant, and within remnants, certain regularities of the radio morphology of many shell-type SNRs are apparent. Relatively young remnants often show a high degree of circular symmetry and, in polarization studies, a radial magnetic field. Others, including older remnants, display some degree of circular or bilateral symmetry in their radio emission. The more evolved SNRs exhibit polarization which indicates tangentially aligned magnetic fields.

We present new radio observations at 843 MHz of two supernova remnants, G296.5+10.0 (PKS 1209−51/52, Milne 23) and G327.6+14.6 (SN 1006, PKS 1459−41), each of which displays a high degree of bilateral symmetry, both in emission intensity and in radial outline. Both are at relatively high Galactic latitudes and, of known remnants, are probably among the most displaced from the Galactic plane.

II. THE NEW RADIO OBSERVATIONS

a) The Telescopes

The observations at 843 MHz were made in 1983 and 1984 with the Molonglo Observatory synthesis telescope (MOST) of the University of Sydney and with the Parkes 64 m radio telescope. The MOST is a synthesis interferometer consisting of two colinear cylindrical paraboloids aligned east-west, each 800 m in extent (Mills 1981). A map is produced in real time by an overlaying of the outputs of a comb of fan beams which track the field center over a period of 12 hr. The synthesized

[1] Visiting Astronomer, Division of Radiophysics, CSIRO, Australia (1983–1984).

half-power beamwidth is 44″ (right ascension) by 44″ csc δ (declination) within a field size of 70′ by 70′ csc δ. The synthesized beam produced by this method has one major sidelobe of roughly −8% intensity, the effects of which are removed from the maps by a special adaptation of the CLEAN technique (Roger *et al.* 1984).

Because of a gap between the east and west paraboloids of the MOST, maps of extended sources are deficient in structure ≥20′. To obtain this structure we have observed the sources with the Parkes telescope which has a half-power beamwidth of 23′ at 843 MHz. The process by which the maps of extended and fine structure are added together has been described elsewhere (Roger *et al.* 1984).

b) The Map of G327.6 + 14.6

G327.6+14.6 was observed in a single 70′ field of the MOST. The half-power beamwidth is 44″ (E-W) by 66″ (N-S). Calibration sources used for the observation and their assumed flux densities at 843 MHz (McAdam and Calabretta, private communication) are listed in Table 1. The calibration source for the lower resolution observations with the Parkes telescope was PKS 1934−63, with an assumed flux density of 13.76 Jy. The total flux density, derived from the Parkes observations alone, is 17.5 ± 1.5 Jy. This value is ~15% less than one would predict from an interpolation of measurements at various frequencies made in the period 1965–1970 (Milne 1971). However, the uncertainties of the interpolated value and of our measurement are such that we would judge this difference to be of only marginal significance.

Figure 1 shows the contour map of the remnant from the combined observations. From the extent to which the broad depression inherent in the synthesis observations (due to the missing short-spacing visibilities) is removed and from the agreement of the total flux in the final map with that of the

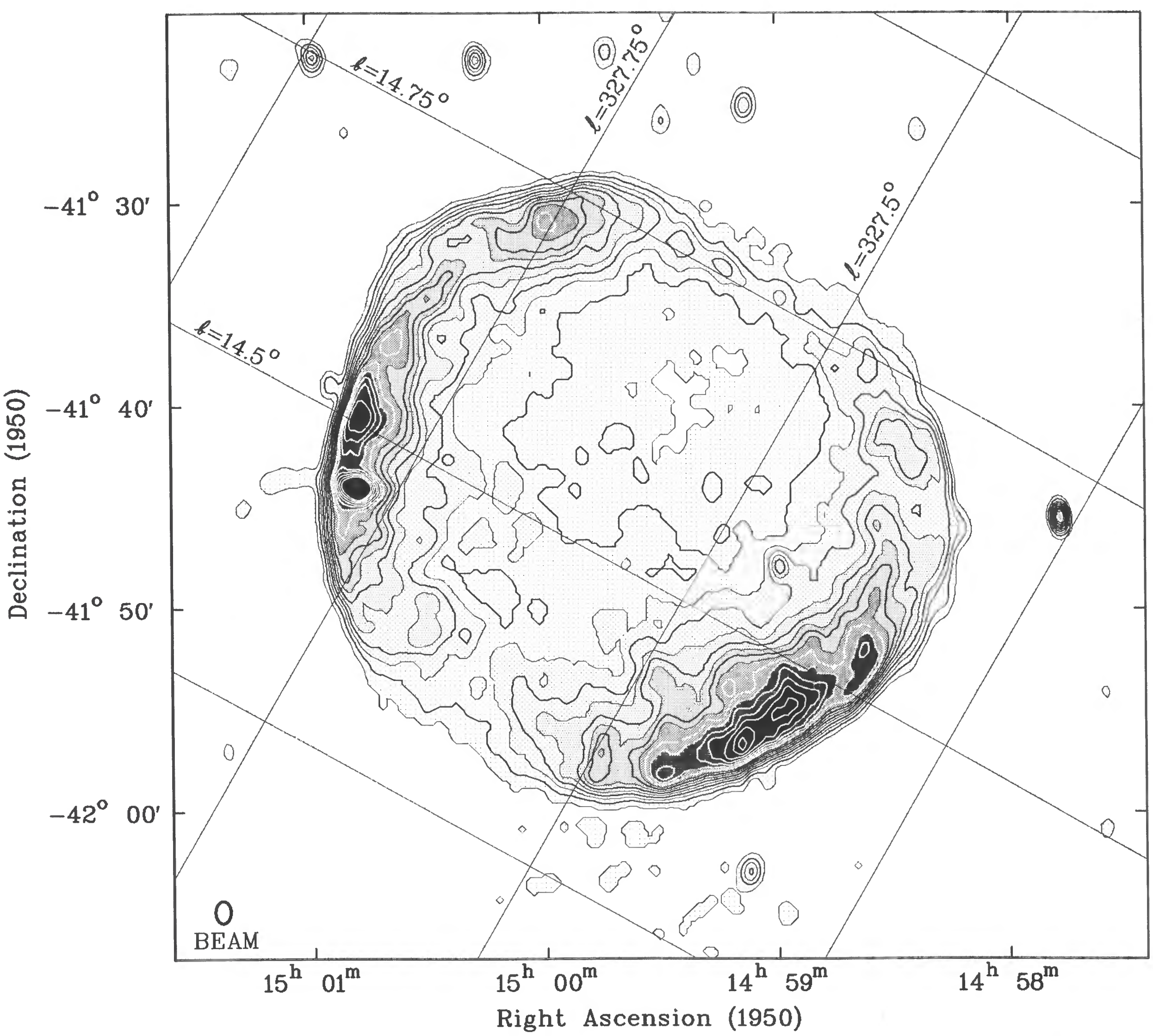

FIG. 1.—The 843 MHz map of G327.6 + 14.6 from combined Molonglo and Parkes observations. Contours are at intervals of 6 mJy per beam area from 6 to 96 mJy per beam area. The first white contour is 60 mJy per beam area. The synthesized half-power beam (44″ × 66″) is shown in the lower left corner.

TABLE 1

CALIBRATORS USED FOR "MOST" OBSERVATIONS

		FIELD					
CALIBRATOR	FLUX DENSITY (Jy)	G327 (1984 Aug 8)	G296 NE (1984 Feb 11)	G296 NW (1984 Feb 12)	G296 SE (1983 Oct 9)	G296 SW (1984 Feb 10)	G296 S (1984 Apr 27)
PKS 0407−65	25.9		×	×		×	×
PKS 0409−75	21.0		×	×	×	×	×
PKS 0833−45	2.63			×		×	×
PKS 0943−76	2.93		×	×	×	×	×
PKS 1143−48	4.26	×					
PKS 1215−45	6.74	×					
PKS 1547−79	5.79				×		
PKS 1814−63	21.2		×	×		×	×
PKS 1827−36	13.8	×					
PKS 1934−63	13.7	×	×	×	×	×	×
PKS 2150−52	5.47		×		×	×	×

single dish measurement, we estimate that the merging process is accurate to approximately ±10%.

The map closely resembles a recent 1.37 GHz map made from observations with the Very Large Array (Reynolds and Gilmore 1986). Our observations confirm features noted on previous observations of lower resolution (Stephenson, Clark, and Crawford 1977) and of lower sensitivity (Caswell *et al.* 1983). The improved sensitivity permits better definition of the steep outer boundaries near the regions of the shell with the highest emission, and shows the absence of such a steep boundary adjacent to the low-level emission on the northwest and southeast perimeters. Emission in the central region is weak, with a minimum just northwest of the center.

The emission shows pronounced bilateral symmetry both in outline and in emission intensity. The axis of symmetry is oriented at position angle −34° and is offset from a line of constant Galactic longitude by −4°. The degree of symmetry in the radial outline of the emission is illustrated in Figure 2 in which an outer contour of emission (6 mJy per beam area) is shown together with its image reflected about the axis. As a fraction of the mean radius, the rms difference between the two is 3.5%.

The degree of symmetry in emission intensity is illustrated in Figure 3 in which we show radial profiles averaged over sectors of width 15° at six position angles from the assumed center of the source ($\alpha = 14^h57^m37^s$, $\delta = -41°44'22''$). The integrated emission in each 30° sector is plotted as a function of the angle from the symmetry axis in Figure 4. Apart from the steep outer edge of emission in directions away from the axis, the bulk of the emission from G327, as seen in projection, is not resolved into fine-structure components.

Finally, we draw attention to the low-level spur of emission extending ~2'.5 from the east side of the source. Reynolds and Gilmore (1986) suggest that this feature is not part of the remnant but is probably related to the bright point source of emission near the maximum of the shell emission which they have identified with an elliptical galaxy of about 16th magnitude.

c) The Map of G296.5+10.0

Observations with the MOST of four 70' fields were required to fully cover the extent of G296. Observations of a fifth field were subsequently undertaken to determine the extent of low-level emission in the south central region of the remnant. The calibration sources and their assumed flux densities used for the various fields are listed in Table 1. Our final map comprises the mosaic of these five fields and the short-spacing data taken from the map made with the Parkes telescope and calibrated using PKS 0915−11 with an assumed flux density at 843 MHz of 70.0 Jy. This map, shown in Figure 5, is therefore complete in structure down to the scale of the half-power beamwidth of 44'' (E-W) by 56'' (N-S). The extended structure from the Parkes observation is apparent as low-level emission along the symmetry axis of the remnant, in the central regions of the source, and as an enhanced background in regions of the bright filamentary structure on the east and west sides.

The total flux density from G296 is 59 ± 2 Jy, a value largely dependent upon the observations with the Parkes telescope. The agreement of the total flux density in the final map with that in the Parkes map alone indicates that the merging

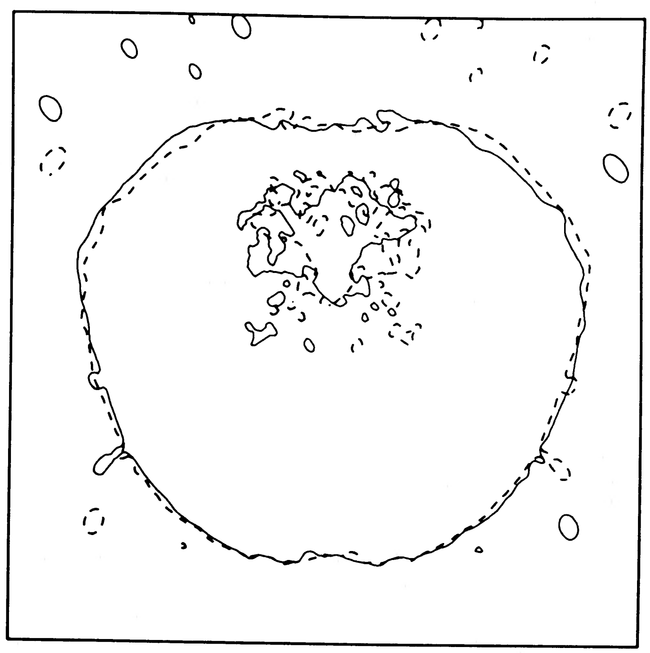

FIG. 2.—Outer contour (6 mJy per beam area) from the map of G327.6+14.6 (*solid line*) superposed with an image of the contour reflected about the axis of symmetry (*dashed line*). Note the high degree of symmetry in the radial outline.

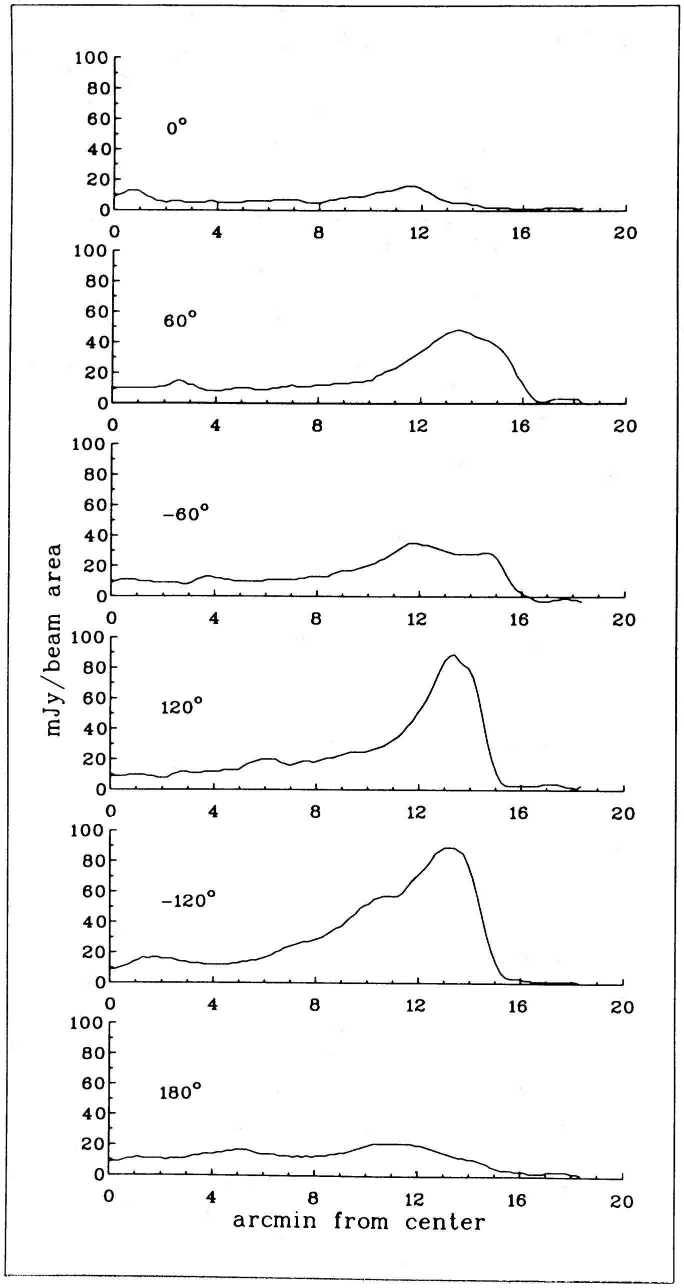

FIG. 3.—Radial profiles of the emission from G327.6+14.6 averaged over 15° sectors centered on the indicated position angles which are measured from the (northern) axis of symmetry.

process is accurate to within $\pm 12\%$. There are ~ 30 point sources (presumably extragalactic) stronger than 6 mJy within the area of emission from the SNR which contribute slightly less than 1 Jy to the total flux density.

The emission from G296 also shows strong bilateral symmetry, although to a lesser extent than that from G327. The axis of symmetry is at position angle 2°.5, and is inclined by only 7° from a line of constant longitude. As with G327, the emission from the shell is strongest in the southeast and southwest flanks, with very low-level emission along the axis. Some aspects of the emission are, however, quite different from those of G327. First, the radius of curvature of the east shell is distinctly less than that of the west, suggesting a center of expansion to the east of the geometric center (see § III*b*). Second, the outline of the emission shows pronounced extension along the axis direction. In Figure 6 we illustrate the variation in the radius of the outline of emission (from an assumed center of symmetry $\alpha = 12^h06^m45^s$, $\delta = -52°04'44''$) with the angle from the axis. Third, there is a sharp decline in emission in the southeast and southwest at an angle either side of the axis of $\sim 18°$. Finally, much of the emission is fragmented, containing substantial fine structure in the form of long thin filaments elongated tangentially to the outline of the shell. These last two features are illustrated in Figure 7 in which we show a gray-scale image of the remnant from the synthesis observations alone, before the addition of the Parkes data. This map, which lacks components of emission broader than $\sim 20'$, emphasizes the "filamentary" nature of much of the radio emission. The filaments are largely confined to the outer third of the radius. Figure 8*b* shows eight perpendicular cuts through the emission at angles and positions illustrated in Figure 8*a*. Measurements of the width of a number of filaments show that most appear to be resolved or partially resolved by the synthesized beam with widths falling in the range 0'.4–1'.2.

III. OTHER OBSERVATIONS AT RADIO, OPTICAL, AND X-RAY WAVELENGTHS

a) *G327.6+14.6*

Measurements of the polarization of the 2.7 and 5.0 GHz radio emission with the Parkes telescope (Milne 1971; Milne and Dickel 1975) have shown the emission regions of G327 to have a radially aligned magnetic field component which is characteristic of young supernova remnants (Dickel and Milne 1976). This suggests that the radio emission in young remnants is mainly due to a process other than simple compression of the ambient field. The moduli of the rotation measures for the source are typically ≤ 25 rad m^{-2} in the regions of intense emission.

Detected optical emission from the SNR is confined to faint filamentary arcs visible in the Balmer lines of hydrogen (van den Bergh 1976) on a short section of the northwest periphery near the axis of radio and X-ray symmetry. Hesser and van den Bergh (1981) have subsequently measured a proper motion in the filaments of 0''.39 per year. Recent observations of Kirshner, Winkler, and Chevalier (1987) reveal a broad component to the Hα emission due to charge exchange between hydrogen atoms and shock-heated protons. The width of this component implies a shock velocity in the range 2800–3870 km s^{-1}. For the atomic component, Kirshner *et al.* (1987) deduce a preshock density of ~ 0.02 cm^{-3}. It is interesting that no optical emission has been detected either from the east or west sides, bright in radio emission, or from the corresponding axial region to the south.

Wu *et al.* (1983) have reported highly broadened absorption lines of Fe^+ against the continuum emission of a background sdOB star in the direction of G327. The line widths suggest Doppler broadening with velocities of 5000–6000 km s^{-1} which the authors ascribe to freely expanding ejecta.

Images of the X-ray emission from G327 measured with the IPC of the *Einstein Observatory* are described by Pye *et al.* (1981). For the energy range 1–4 keV the distribution is similar to that of the radio map, with strong shell emission and bilateral symmetry about an axis perpendicular to the Galactic plane. X-rays in the lower energy range (0.1–0.3 keV) are more

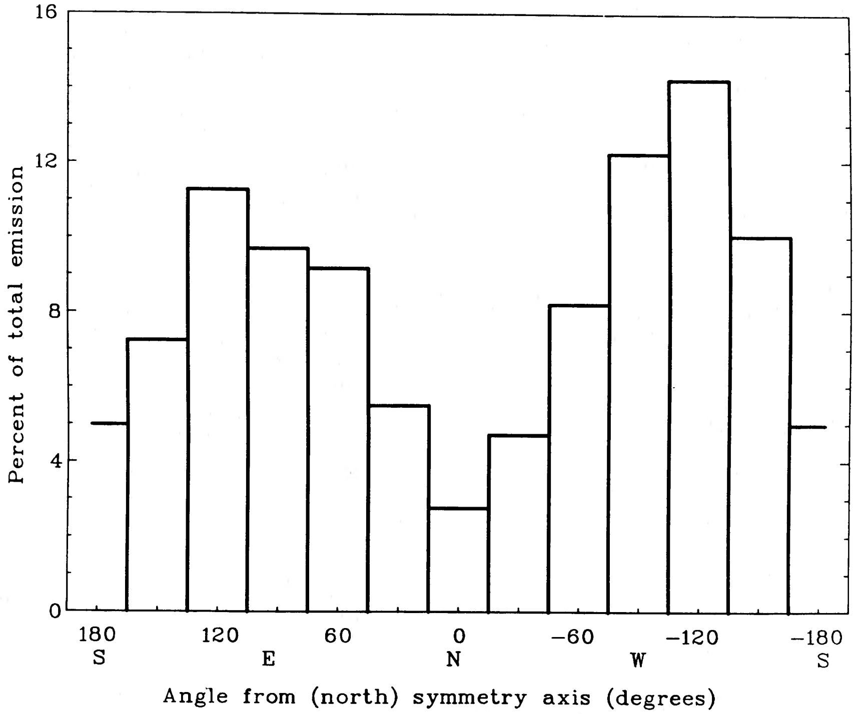

FIG. 4.—Integrated emission in each 30° sector of G327.6 + 14.6 as a fraction of the total emission. Abscissa indicates the position angle of the sector measured from the (north) symmetry axis.

uniformly distributed over the area of the source. Recently Vartanian, Lum, and Ku (1985) have detected line emission from O VII and O VIII near 0.6 keV with rocket instruments, confirming an earlier detection of excess emission below 1 keV by Galas, Venkatesan, and Garmire (1982).

b) G296.5 + 10.0

Early low-resolution maps of the emission at 1.4 and 2.65 GHz from G296 by Whiteoak and Gardner (1968) showed 15%–25% linear polarization with alignments which implied a magnetic field in the emitting regions tangential to the shell circumference. Later measurements with the Parkes telescope at 5 GHz (Milne and Dickel 1975) confirmed this field orientation and low values of rotation measure (-20 to 40 rad m^{-2}). The rotation measure is positive in the eastern lobe and negative on the western side. In contrast to G327, the tangential field alignment in G296 is characteristic of more evolved supernova remnants (Dickel and Milne 1976).

Optical emission from G296 was first detected by Irvine and Irvine (1974) in Hα and in [O II] at 3727 Å. We have indicated the positions of these filamentary nebulosities with hatching in Figure 7. It is clear that, although one area of nebulosity is in the general direction of radio emission in the southwest quadrant, none of the filaments is coincident with a radio filament. Spectrograms taken by Ruiz (1983) at three positions in filaments in the most northerly area of nebulosity show numerous lines with some variation in relative strengths. According to Ruiz, line ratios of [S II] indicate densities near 5 cm^{-3}, while all temperature sensitive ratios indicate values in excess of 2.5×10^5 K.

X-ray emission from G296 observed with the IPC of the *Einstein Observatory* has been reported by Helfand and Becker (1984) and described by Matsui, Long, and Tuohy (1988). More recent observations with *EXOSAT* have been reported by Kellett *et al.* (1987). As with G327, the total emission in the band 0.1–4.0 keV shows an overall resemblance to the radio emission, with the most intense X-ray emission coming from the same general regions in the southwest and southeast which emit most strongly in the radio. On the east side the emission extends northward to the northeast quadrant following the filaments of radio emission. By contrast, however, the radio emission in the northwest quadrant shows no detectable X-ray counterpart. There is also no X-ray emission observed from regions on the perimeter close to the axis of symmetry.

A remarkable feature of the X-ray emission from G296 is the compact source near the center of the remnant. The position of this source is marked in Figure 5. The object was first detected with the *Einstein* IPC and was described by Helfand and Becker (1984), who, because of the high probability (~4%) of finding a background source somewhere within the whole area of the remnant, suggested that it was probably unrelated. However, Kellett *et al.* (1987) point out that the probability of finding an X-ray source within 8′ of the center of the remnant is very low and, after considering other identifications and the parameters expected for an X-ray source of the age of the SNR, favor a neutron star interpretation for the point source. The displacement of the compact source from the geometric center is toward the east shell which, in radio emission, shows a smaller radius of curvature than the west shell (see § II*c*). If the remnant has expanded from the position of this compact source, then the smaller radius would be consistent with the eastern shell having a lower average velocity and possibly encountering greater deceleration.

We have searched our map for a radio counterpart to this X-ray source and set an upper limit to its flux density at 843 MHz of 3 mJy. Searches for pulsed radio emission

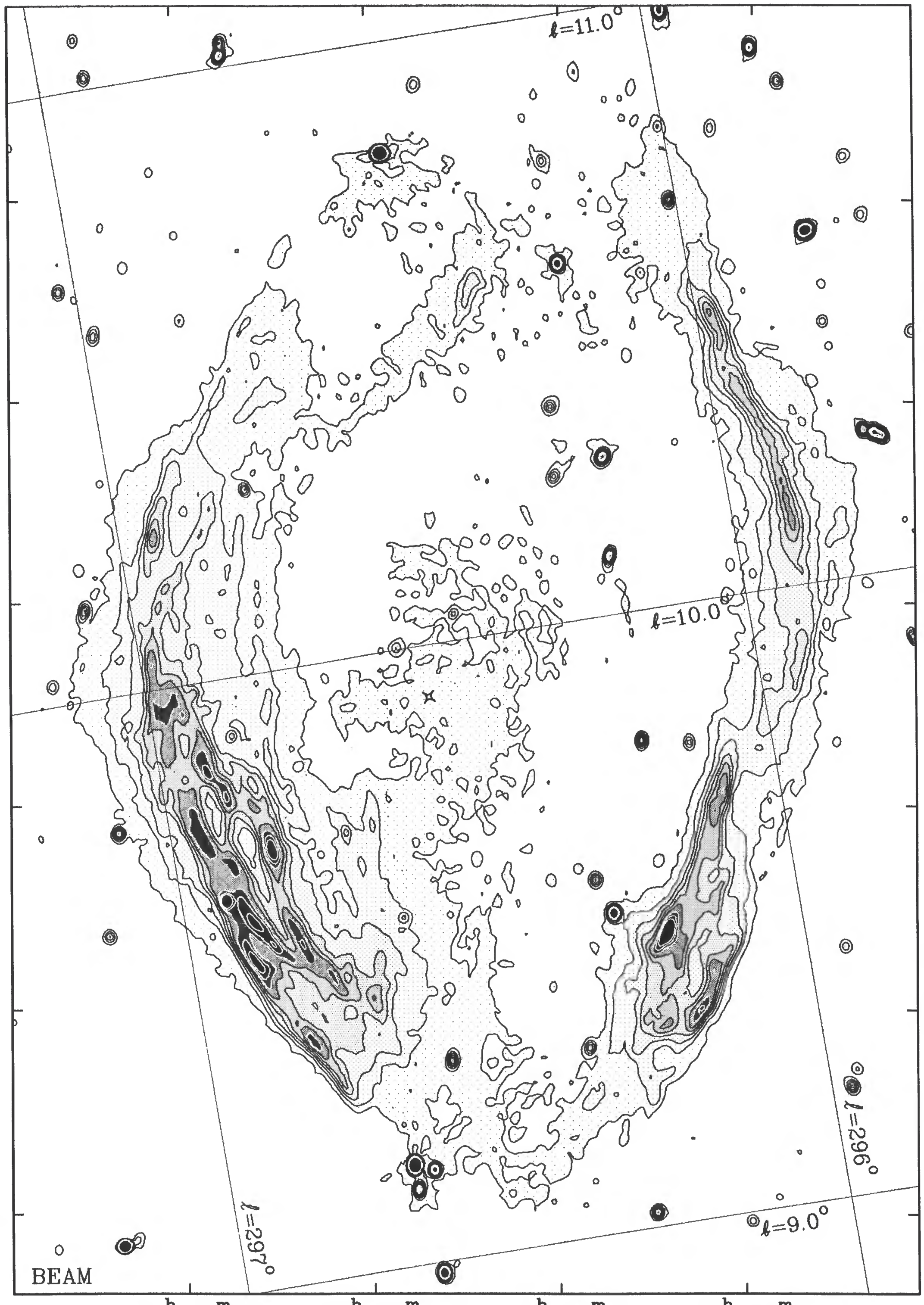

FIG. 5.—The 843 MHz map of G296.5+10.0 from combined Molonglo and Parkes observations. Contours are at intervals of 6 mJy per beam area from 4 to 52 mJy per beam area. The first white contour is 40 mJy per beam area. Synthesized half-power beam (44″ × 56″) is shown in the lower left corner. Open-centered " ×," 6′ southeast of the map center, marks the position of the compact X-ray source, EXO 120723−5209.8.

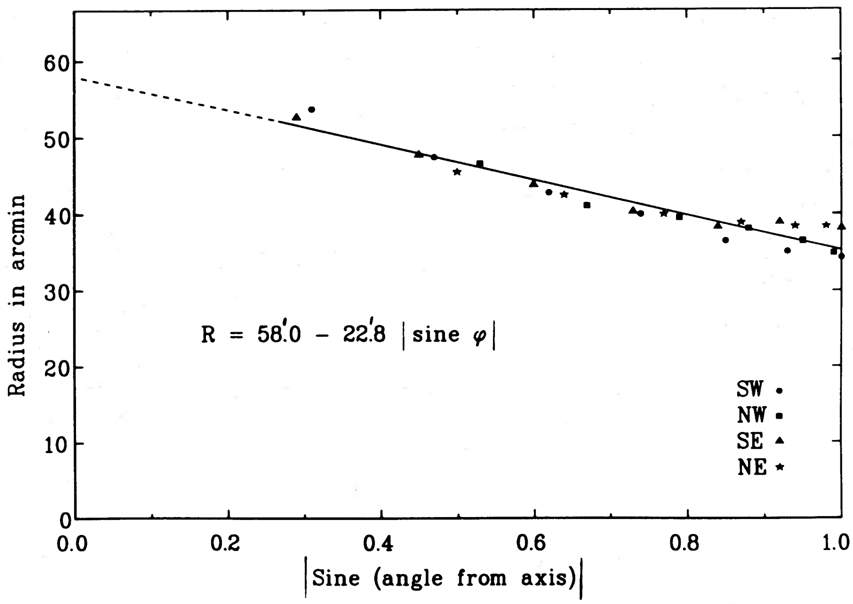

FIG. 6.—Radius of the outer emission boundary of G296.5 + 10.0, measured from the assumed center as a function of the modulus of the sine of the angle from the axis of symmetry. Quadrant for each measured radius is coded by the symbols as shown. The equation for the best-fitting line to the points is indicated.

(Manchester, D'Amico, and Tuohy 1985) have also been unsuccessful.

IV. ESTIMATES OF PHYSICAL PARAMETERS

a) *G327.6 + 14.6*

The age of this remnant follows from its association with the chronicled event of 1006 AD (Gardner and Milne 1965) which is now well established (Stephenson, Clark, and Crawford 1977). Kirshner, Winkler, and Chevalier (1987) combine their estimate of shock velocity with the measurement of the proper motion of the Hα filament (see § III*a*) to determine a distance of 1.8 ± 0.3 kpc to G327. This value is close to that found by Hamilton, Sarazin, and Szymkowiak (1986) to be compatible with a model to the X-ray emission comprising a blast wave plus a reverse shock in an ejecta plasma rich in carbon and heavy elements.

At a distance of 1.8 kpc, the remnant would have a radius of 7.8 pc and would be located 450 pc above the galactic plane. At this location we might expect the ambient gas to be dominated by the diffuse, largely ionized component (Mathis 1986) with a density close to the value of 0.05 cm^{-3} used in the X-ray model of Hamilton *et al.* (1986). Swept-up material would amount to 3.7 $M_\odot$, which would imply that the remnant is still in transition from free expansion to the adiabatic Sedov-Taylor phase. For an initial ejecta mass of 1.4 $M_\odot$ with energy of 1.0×10^{51} ergs, the present blast wave velocity would be 4200 km s^{-1}, slightly larger than that estimated by Kirshner, Winkler, and Chevalier (1987).

b) *G296.5 + 10.0*

The distance to G296 is not well determined. Σ–*D* estimates, corrected for *z*-distance, yield values of 1.1 kpc (Milne 1979) and 1.9 kpc (Caswell and Lerche 1979). Recent observations of the H I distribution in the direction of G296 with a resolution of 34′ (Dubner, Colomb, and Giacani 1986) show no features in the neutral gas which can be related with any certainty to the supernova remnant. However, the authors suggest an association with a "peanut-shaped" depression in gas with v_{lsr} in the range −11 to −17 km s^{-1}. In projection this feature partially surrounds G296 and extends to the position of another nonthermal source, G300.1 + 9.4. For most models of Galactic rotation, these velocities are consistent with a distance to G296 in the range 1–2 kpc.

An inspection of the latitude-velocity contours of H I emission in the direction of G296 (e.g. Kerr *et al.* 1987) indicates that virtually all the extended emission is from distances substantially closer than the tangent point ∼4 kpc away. Estimates of the thickness of the mean H I disk at this longitude (e.g., Jackson and Kellman 1974; Celnick, Rohlfs, and Braunsfurth 1979) suggest that ∼90% of the distributed H I will be within 220 pc of the plane or at a distance of less than 1.3 kpc. From Kerr *et al.* (1987) and Dubner, Colomb, and Giacani (1986) the mean total column density of H I through the Galaxy in the direction of G296 is 1.2×10^{21} atoms cm^{-2}. By comparison, Ruiz (1983) has measured the obscuration of the north-central optical filament of G296 to be $A_v = 0.5$ mag which implies a total hydrogen column density (Bohlin, Savage, and Drake 1978) to the remnant of $\sim 1.0 \times 10^{21}$ atoms cm^{-2}. This is close to the value of absorbing column density required to fit the *EXOSAT* X-ray spectrum of $\sim 1.4 \times 10^{21}$ cm^{-2} (Kellett *et al.* 1987), but somewhat less than the $\sim 3.2 \times 10^{21}$ cm^{-2} estimated from the *HEAO 1* data (Tuohy *et al.* 1979). A similar comparison has led Kellett *et al.* (1987) to conclude that G296 is probably beyond most of the Galactic H I emission, as would be the case for a distance in excess of 1 kpc. It should be remembered, however, that the X-ray estimates of total (H I, H II, and H_2) column density have considerable uncertainty, and that the comparison is with a mean H I disk distribution which may not be applicable to one specific direction. Nonetheless, the distance estimates are loosely constrained by the column density estimates on the low side (∼1 kpc) and by the plausible extent of Galactic material (∼2 kpc) on the high side.

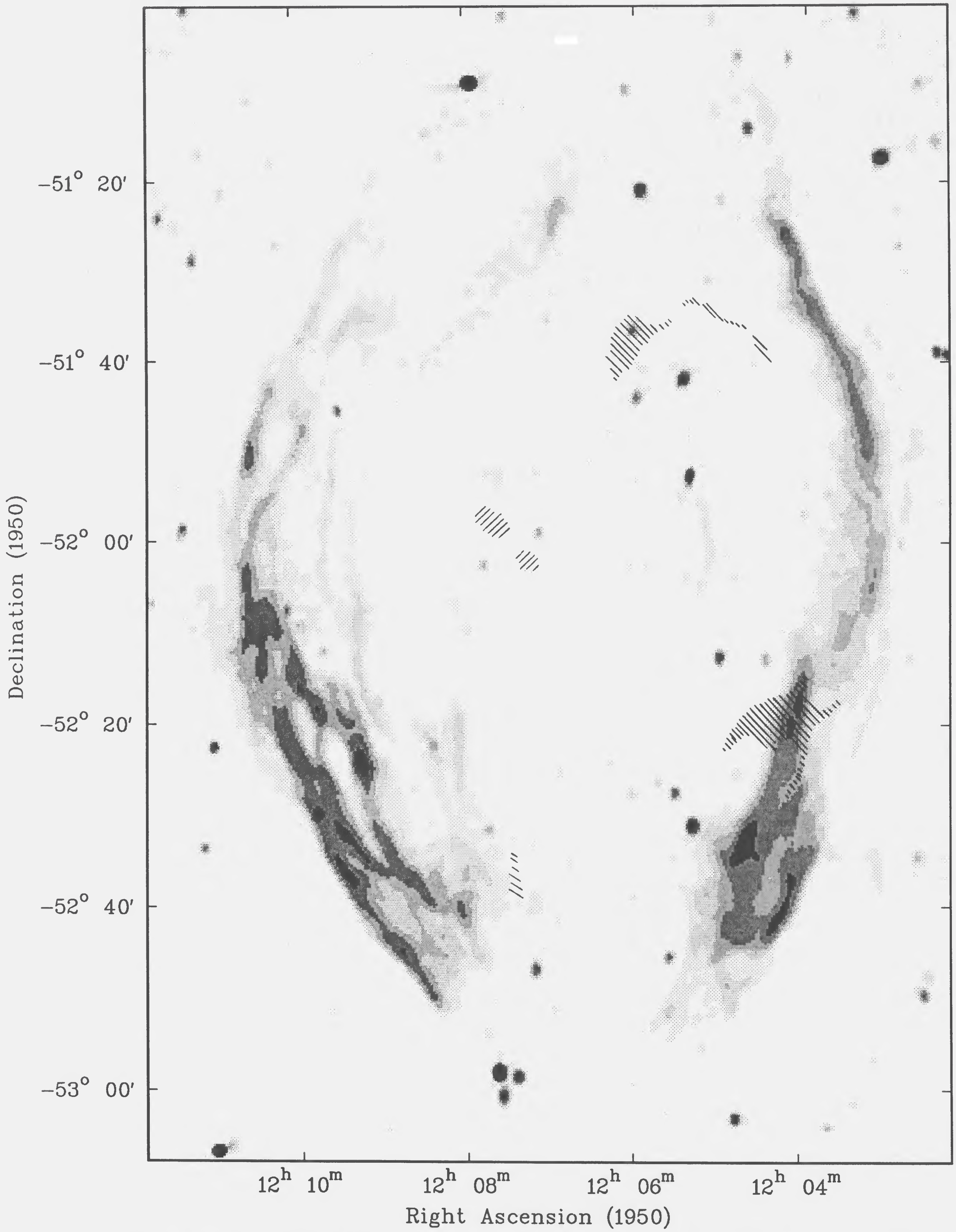

FIG. 7.—Gray-scale image of G296.5+10.0 from the MOST observations alone. Note the filamentary structure, made more apparent by the absence of extended emission, and the well-defined southern gap in the emission ~18° either side of the axis of symmetry. Nebulosity visible in the ultraviolet and Hα (Irvine and Irvine 1974) is shown as hatching with a negative slope; that visible only in Hα is indicated with positively sloped hatching.

The estimation of the age and shock velocity for remnants in the adiabatic phase requires some knowledge of the density of the most pervasive intercloud component, the initial kinetic energy, and the size of the remnant. The mean ambient particle density near G296, from the X-ray data, is estimated to be 0.24 cm^{-3} by Kellett *et al.* (1987) and 0.08 cm^{-3} by Matsui, Long, and Tuohy (1988). This latter value is close to the density expected from the sum of the mean disk distributions of H I and H II at a distance of 1.5 kpc. Both values are significantly less than the cloud density of 5 cm^{-3} estimated from optically emitting filaments (Ruiz 1983). Using combinations of these two intercloud density values with radii equivalent to distances of 1 and 2 kpc and an initial kinetic energy of 6×10^{50} ergs (Kellett *et al.* 1987), we estimate a mean age for G296 of 7000 yr with an uncertainty of a factor of 3 and a mean blast wave velocity of 800 km s^{-1} with an uncertainty of a factor of 2. Despite these large uncertainties, the values are consistent with the remnant being in an adiabatic expansion phase.

V. THE SIGNIFICANCE OF THE BILATERAL SYMMETRY

The dominant feature of the radio and X-ray emission from these two high-latitude remnants is the symmetry, in peripheral outline and in emission intensity, about a well-defined axis. Many other remnants show a similar symmetry, but usually to a lesser extent. Kesteven and Caswell (1987) find that some degree of bilateral symmetry can be discerned in the radio emission of more than 60% of Galactic remnants. They estimate that this fraction is close to what one might expect if nearly all shell remnants have a cylindrical or "barrel" symmetry in three dimensions which manifests itself in projection as bilateral symmetry if a large enough angle exists between the cylinder axis and the line of sight. The property is sufficiently prevalent among both young and old remnants that one must search for either (i) an underlying single cause which persists throughout the lifetime of a remnant, independent of its type, or (ii) multiple causes which, depending upon the age of the remnant and the region into which it is expanding, separately impose symmetry on the observed emission and outline.

The case for multiple explanations is based on two main arguments. First, the environment into which a supernova derived from a massive progenitor (Type II or Ib) expands is likely to be significantly modified by radiative and wind effects during the star's lifetime. Emission from remnants of such supernovae thus may be considerably affected, even at times dominated, by conditions in and surrounding any bubble formed by the progenitor. Second, as we have previously noted, observations of the polarization of radio emission show that the magnetic field orientation is distinctly different in the postshock regions of young and old remnants. The emission distribution in G296 may be the result of expansion into the boundaries of a preformed bubble generated by a stellar wind or H II region of a massive precursor as has been suggested to explain emission related to HB 21 and W44 (McKee, van Buren, and Lazareff 1984), N49 (Shull *et al.* 1985) and IC 443 (Braun and Strom 1986). Studies by Lasker (1966) have shown that under certain conditions an H II region may expand aspherically and leave behind a prolately ellipsoidal bubble into which a remnant such as G296 might expand. The bilat-

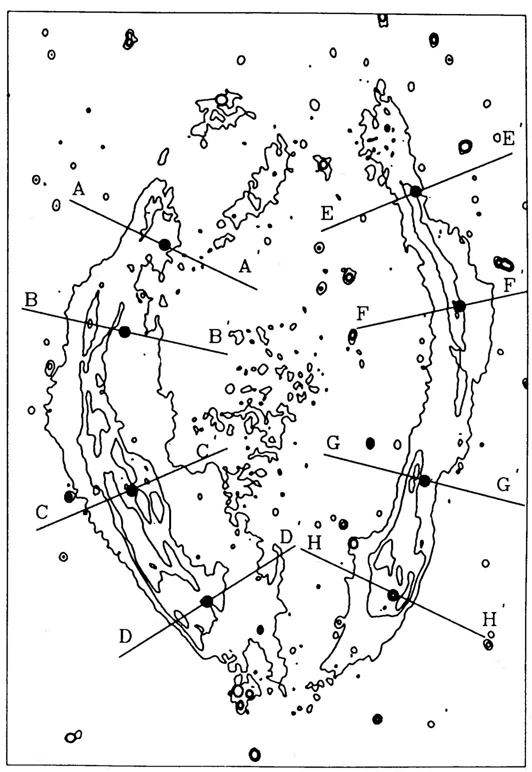

FIG. 8*a*

FIG. 8.—(*a*) Positions of eight perpendicular cuts (*solid lines*) and their centers (*filled circles*) relative to a few contours from the map of G296.5 + 10.0 (cf. Fig. 5). (*b*) Intensity of the emission as a function of the angular displacement from the center of each cut.

eral symmetry in emission might then arise from a higher deposit of energy per unit area on those parts of the bubble closest to the explosion center. If the prolate shape of the postulated bubble is due to the orientation of the ambient magnetic field (i.e. the bubble is extended in the direction of the field lines), then a compressed field in the equatorial region of the bubble or its shell may also enhance the radio emission. A prolate bubble could also arise around a massive star centrally placed in a layer of enhanced gas density.

For remnants such as G327, which is almost certainly a remnant of a Type I event (see Hamilton, Sarazin, and Szymkowiak 1986), there is little possibility that the symmetry in emission or in outline has been influenced by a precursor bubble. Instead, the age of G327 would suggest that its emission characteristics may still be influenced by a nonisotropic outburst of ejecta. The supernova model of Bodenheimer and Woosley (1983) for *massive* rotating stars predicts mass ejection initially centered in the equatorial plane and remnants with toroidal symmetry as a possible outcome. It is relevant to question whether or not Type I explosions of accreting white dwarfs could show a similar effect.

Kesteven and Caswell (1987) postulate that such toroidal outbursts may be the underlying cause of bilateral symmetry in most remnants which show this property. Other than a detailed modeling of various types of supernova events which might lend credence to this hypothesis, it is difficult to envisage tests which would confirm or deny this possibility. We note, however, that, given a homogeneous surrounding medium, Bisnovatyi-Kogan and Blinnikov (1982) find that the shock front of an initially asymmetric explosion will eventually become spherical through interaction with the medium. Thus, although we might ascribe the bilateral emission symmetry of G327 and G296 to an initial ejection toroid, the latter remnant's extension along the axis of symmetry would still require a separate explanation.

Bilateral symmetry in the radio emission from SNRs has long been ascribed to the alignment of the magnetic fields in the regions into which remnants are expanding through compression of the magnetic field in directions where the shock is propagating transverse to the field lines (van der Laan 1962; Whiteoak and Gardner 1968; Shaver 1969). In addition Caswell (1979) and Shaver (1982) have detected a tendency for

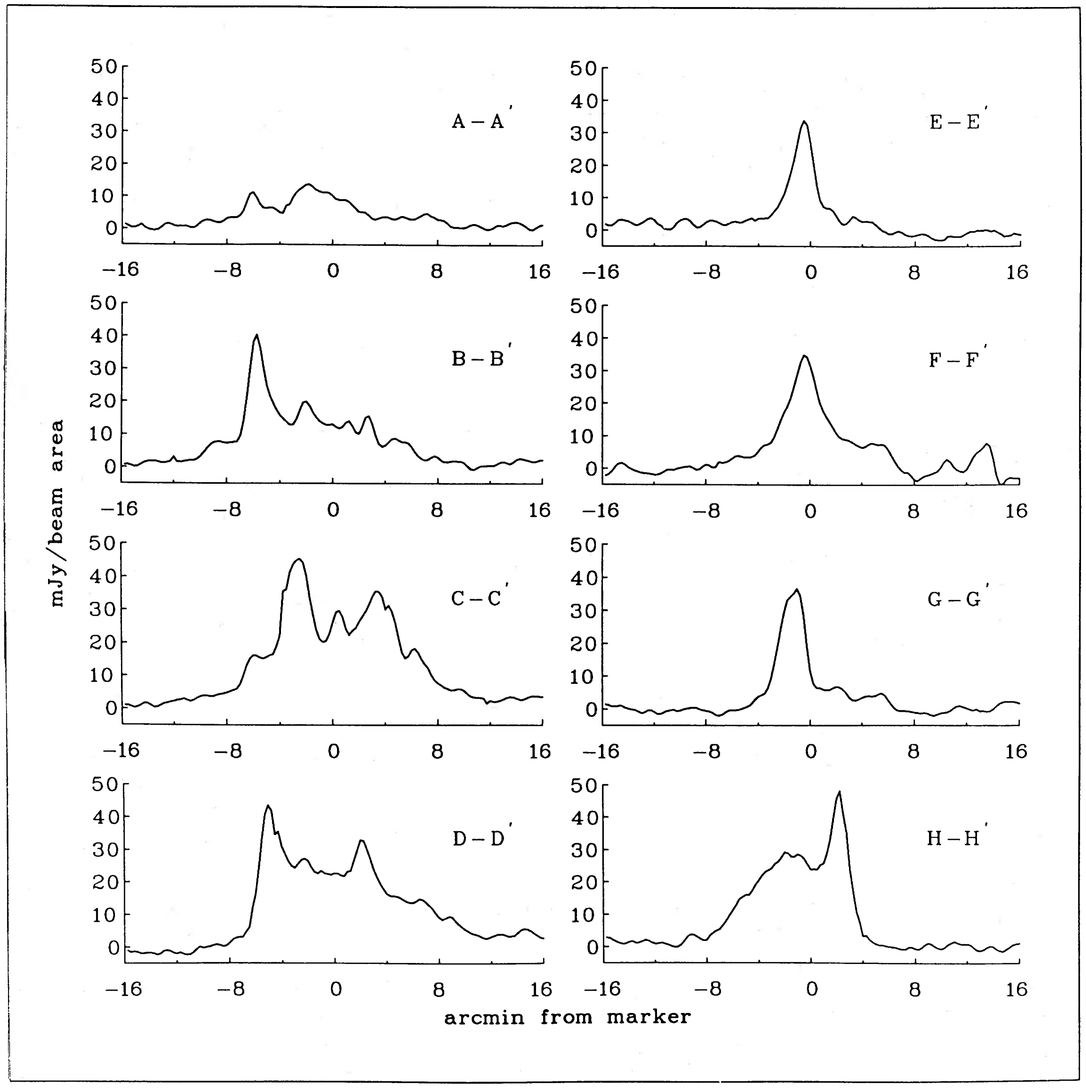

FIG. 8*b*

filled-center remnants to be elongated in the Galactic plane, supposedly along the direction of the magnetic field. It is unlikely that simple field compression alone is sufficient to account for the variation in emission in shell remnants, and, as we have noted in § III*a*, such an explanation is at variance with the observations of radially aligned fields in the postshock regions of young remnants such as G327. There are, however, other aspects of collisionless shock propagation which may be relevant to the efficiency of the generation of emitting particles, both in the radio and at other wavelengths. In the next section we consider the possibility that the direction of propagation of collisionless shocks relative to the magnetic field orientation in the ambient preshock medium influences both the acceleration of radiating particles at the shock front and the shocks' ability to couple to incoming ions. In proposing this explanation as a single underlying cause of bilateral symmetry in remnants, we rely heavily on the recent work of Jokipii (1987) which actually predicts that the rate of acceleration of relativistic particles in shocks will be a strong function of the angle to the field direction in the upstream medium.

The detection of any symmetry which results from magnetic field alignment would depend upon there being a significant component of the field perpendicular to the line of sight. For the remnants G327 and G296 the projected axes of symmetry deviate from being normal to the Galactic plane by only 4° and 7°, but we have no knowledge of the deviation in an orthogonal plane containing the line of sight. We have searched without success for possible evidence of the projected field orientation near the remnants in the form of stellar polarization features (Ellis and Axon 1978; Mathewson and Ford 1971) or large scale H I distributions (Colomb, Poppel, and Heiles 1980). In general, however, field-aligned loops emerging normally from the plane are not uncommon as features of polarization or H I emission, and there would appear to be no compelling evidence against such field directions in the neighborhoods of these remnants.

VI. THE INFLUENCE OF THE INTERSTELLAR MAGNETIC FIELD ON THE EVOLUTION OF THE REMNANTS

It is generally accepted that coupling of the ejecta of a supernova to the interstellar gas occurs through the scattering and reflection of interstellar ions in the turbulent convection zone associated with the collisionless shock front. The process is thus intrinsically dependent upon the magnetic field and upon the ionization of the preshock gas. Scaled laboratory experiments (Borovsky *et al.* 1984) confirm that, in the absence of a field, no coupling to an ambient plasma will occur. One would normally expect the hot, low-density component which makes up a substantial fraction of the interstellar medium (e.g., McKee and Ostriker 1977) to be mostly ionized, especially at locations with relatively high z-distances in the Galactic plane. Furthermore, for shock velocities in excess of 110 km s^{-1}, UV radiation from the hot shocked gas itself is expected to ensure complete ionization ahead of the shock (Shull and McKee 1979).

Treatments of the dynamics of an expanding remnant which have included the additional pressure due to a compressed magnetic field in the postshock gas (Kulsrud *et al.* 1965; Chevalier 1974) show that, although it may limit the maximum density in the shocked gas, the field should have very little effect on the dynamics (i.e. velocity) of the shock itself. However, measurements of collisionless shocks in the Earth's magnetosphere and in interplanetary space (e.g. Bame *et al.* 1979) indicate a clear difference in morphology between shocks propagating primarily across (quasi-perpendicular) and those moving primarily along field lines (quasi-parallel). In the latter case, the transition in magnetic field and flow velocity from the unshocked medium to the compressed, turbulent heated flow is greatly broadened and lacks the clear discontinuity of the quasi-perpendicular shock.

We propose that, in the collisionless shocks of much higher Mach number that characterize supernova remnants, a similar difference exists between the shocks propagating across and along field lines. We propose that this difference manifests itself (i) in an inability of a quasi-parallel shock to couple efficiently inflowing upstream ions to the postshock gas, (ii) in its relative inability to heat the gas to produce thermal X-radiation, and (iii) in the shock's inability to accelerate the electrons to the relativistic energies required to generate the radio synchrotron emission.

Recent work by Jokipii (1987) indicates that the rate of acceleration of relativistic particles is a strong function of the angle between the shock normal and the upstream magnetic field direction. Jokipii contends that the acceleration in quasi-perpendicular shocks may be much more efficient than previously estimated because the particles will drift along a shock face colliding with it many times in one scattering mean free path. In the following discussion of each remnant we will assume that the symmetry of the radio emission can be explained by the resulting field-shock angle dependence of the synchrotron emission from the electrons subject to on-going acceleration in the neighborhood of the shocks.

a) Early Evolution of SNRs and G327.6 + 14.6

The peak brightness temperatures of the mean radio emission from G327, as depicted in the sector-averaged radial profiles of Figure 3, show an order-of-magnitude variation around the periphery of the source. The overall symmetry of this variation is similar to that of the X-radiation in the range 1.2–4.0 keV (Pye *et al.* 1981). If the radio symmetry is indeed due to the field alignment as outlined above, then either this component of the X-ray emission is synchrotron radiation (see Reynolds and Chevalier 1981) or the conditions in and behind the on-axis (quasi-parallel) shock are, in some other way, less effective in heating the particles in this energy range. By contrast, emission in a lower energy range (0.1–0.3 keV) (Pye *et al.* 1981) may be of a different origin, the mean brightness being much more uniform within the outline, both radially and azimuthally.

In both X-rays and radio, the radial outline of G327 is close to circular, with a slight but definite "apple-shape" departure. The brightest parts of the radio emission are behind the flattened portions of the outline displaced slightly from the center toward lower latitudes. In the context of our interpretation of the emission being most intense in directions where the shock is propagating normal to the ambient magnetic field, the morphology implies that the field lines in the region of the source diverge towards higher latitudes. The "flattening" of the outline at these points would indicate enhanced, relatively recent deceleration of the shell. From the estimates of swept-up mass (see § IV*a*), however, we would expect the remnant to have been ejecta-dominated over most of the past 1000 yr and thus to show only slight departure from circular symmetry in its radial boundary.

b) Later Evolution of SNRs and G296.5 + 10.0

The radio emission from G296 also shows greatest intensity from the east and west flanks, peaking on the lower latitude side of center. The emission is extremely weak on the axis both to the north and south, and it is difficult to say whether or not a shock front actually exists within 10° of the axis. The effect is equally pronounced in the X-ray emission. Again we suggest that the emission is strongest where the shock is propagating transverse to the field and coupling well to the interstellar material. As with G327, the lack of both radio and X-ray emission along the axis may indicate the relative ineffectiveness of the quasi-parallel shock in accelerating particles.

In § II*c* we noted the steep decline in peak radio emission along the shell at position angles subtended at the center of the remnant of $\sim 18°$ either side of the symmetry axis on the southern boundary. If the intensity of radio emission is related to the amount of recently swept-up material, a decline of this sort is not likely to be the result of a lacuna in density, occurring as it does near regions of high emission and being symmetrically placed on both sides of the remnant. It is possible that an abrupt transition in the nature of the propagating shock occurs at this angle to the ambient magnetic field. In the classification of hydromagnetic shocks by Bazer and Ericson (1959), just such a transition occurs between fast compressive magnetic shocks of Types 1 and 2 propagating at an angle Θ_c to the field, where

$$\sin \Theta_c = \frac{\gamma - 1}{\gamma} (1 - s_0)^{1/2} .$$

The parameter s_0 is the ratio of the upstream gas pressure to the magnetic pressure or the squared ratio of sound velocity to the Alfvén velocity in advance of the shock, and γ is the adiabatic index.

For Type 1 ("quasi-perpendicular") shocks the angle exceeds Θ_c, and only a single solution to the shock jump conditions is admissible. By contrast, Type 2 ("quasi-parallel") shocks, for which the angle of propagation is less than Θ_c, possess two admissible solutions to the jump conditions. One of these permits gas compression behind the shock front to increase indefinitely without concomitant field compression. If the sharp decline in emission indeed represents this transition, and if $\gamma = 5/3$, we can interpret the critical angle of 18° as yielding

$$s_0 = 4\pi\gamma k \frac{nT}{B^2} = 0.76 ,$$

where k is Boltzmann's constant, and n, T, and B are the particle density, the temperature, and the magnetic field strength in the preshock gas. This implies a ratio $nT/B^2 = 260$ K cm^{-3} μG^{-2} for the interstellar gas at the low-latitude side of the remnant. Such a value is close to what one would calculate for a position in the Galactic plane (i.e. for $z = 0$) with a diffuse component gas pressure ~ 2000 K cm^{-3} (McKee and Ostriker 1977) and a mean magnetic field of ~ 3.5 μG (Thomson and Nelson 1980). This suggests that any large-scale decline of gas pressure with z is accompanied by a corresponding change in magnetic pressure. Lower values of nT/B^2 cause s_0 to approach zero, and the corresponding critical angle Θ_c to tend to a limiting value of 39°.2. The possible wider angle of the emission gap on the high latitude side of G296, although less well defined than the southern gap, would be consistent with such a lower value.

The relationship between the radius of the outline of emission (and hence the probable position of the blast wave) and the angle from the symmetry axis of G296 is illustrated in Figure 6 and implies that the diameter along the axis is ~ 1.6 times that normal to the axis. Since for adiabatic expansion we expect the radius to be proportional to $n^{-1/5}$, a simple interpretation of the variation in radius is that in the axial direction the shock, over the bulk of the remnant's lifetime, has coupled to only $(1.6)^{-5}$ or $\sim 10\%$ of the ambient density (assuming full coupling transverse to the field). The outline of G296 would suggest a continuous variation of coupling efficiency with angle, at least for angles greater than Θ_c.

VII. THE FILAMENTARY EMISSION OF G296.5+10.0

We have noted that the detailed structure of the emission from G296 differs from that of G327 in that some of its emission is broken into fine filaments aligned tangentially with the outer boundary. This difference almost certainly reflects the more evolved nature of G296. The confinement of the filaments to the outer third of the radius indicates that the structures are in reality thin sheets of emission viewed on edge. Their detection is dependent upon there being sufficient column depth along the line of sight through the structure. Parts of sheets aligned at small angles to the line of sight will comprise some of the broader scale emission near the periphery. Those aligned at large angles will contribute to the faint distributed central emission. The polarization measurements at higher frequencies are of insufficient resolution to allow a separation of the polarization in the filaments from that in broader structure; however, polarized emission at 5 GHz (Milne and Dickel 1975) from the northwest quadrant, which is largely from emission in one long filament, indicates that the field within the filament is aligned lengthwise.

The common explanation of filamentary radio structure proposes that the emission is from radiatively cooled, collapsed interstellar clouds of the sort described by Blandford and Cowie (1982). The blast wave, advancing at a rate determined by the most pervasive and tenuous component of the interstellar medium, overtakes dense gas clouds and drives relatively slow shocks into them. The postshock gas eventually cools by recombination and compresses, enhancing the magnetic field and aligning it parallel to the shock front. In most circumstances the compression will be limited ultimately by the increased magnetic pressure. Blandford and Cowie suggest that relativistic electrons within the cloud will be accelerated in the compression process and that this, combined with the enhanced magnetic field, will account for the radio emission.

For this mechanism to be effective, the shocked gas must have been able to cool in a time short compared to the age of the SNR. Following McKee and Cowie (1975), and assuming dynamic pressure equilibrium between the blast wave and the cloud shock, the cooling time τ is given by

$$\tau \approx 4.5 \times 10^{-6} v_{b5}^4 n_0^2 n_c^{-3} \text{ yr} ,$$

where v_{b5} km s^{-1} is the velocity of the blast wave, n_0 and n_c are the particle densities of the ambient medium and of the shocked cloud. For a blast wave velocity of 900 km s^{-1} and an ambient medium density of 0.08 cm^{-3} (see § IV*b*) clouds of initial density $n_c \geq 3$ cm^{-3} should cool in times less than 500 yr and thus satisfy the criterion. We note, however, that optical and near-UV emission from cooling transitions corresponding to these radio filaments has not been detected, and that, unlike the case of a number of SNRs such as IC 443, the few filaments that are detected from G296 (Irvine and Irvine 1974) are not coincident with the radio filaments (see Fig. 7). It seems unlikely that the detection of filaments is severely hampered by obscuration since the particle column density inferred from the X-ray spectrum (§ III*b*) indicates a mean visual extinction of ~ 1 mag.

Blandford and Cowie (1982) suggest that "clouds which have been fully crossed by radiative shocks may be hard to detect optically while remaining as strongly emitting radio regions." In this view G296 would be older, in equivalent evolutionary stage, than SNRs such as the Cygnus Loop which still radiate strongly. Although it is conceivable that some dense clouds within G296 could have cooled completely, it would be very surprising in such a case that more recently shocked clouds on the periphery did not radiate.

We suggest, instead, that the radio filaments may be partially cooled clouds with temperatures near 10^6 K, still too hot to radiate substantially at near-UV and optical wavelengths. Clouds overtaken by shocks of $v \leq 1000$ km s^{-1} will be heated to temperatures $\leq 10^7$ K (Hollenbach and McKee 1979). The clouds may have begun cooling by permitted X-ray transitions in the range 200–1000 eV (Cox and Daltabuit 1971). Concomitant compression may be sufficient to yield filaments of width ~ 0.5 pc ($\sim 1'$) as observed in the radio. By comparison, the filaments observed optically (Irvine and Irvine 1974) show significantly smaller widths, of order 0.1 pc (10″–20″) and no detectable radio emission. The line ratios in these filaments (Ruiz 1983) suggest $T \geq 2.5 \times 10^5$ and densities ~ 5 cm^{-3}. Supposedly the cooling and compressional history of these optical filaments has not been conducive to the enhancement (or even retention) of the relativistic particle densities and/or magnetic field strengths required for radio filaments. Alternatively, since the optical filaments are not positioned on or, with one exception, aligned tangentially to the remnant's radio shell, it is possible that they have been formed through a distinctly different process. Ruiz (1983) speculates that the emitting material may be supernova ejecta.

VIII. CONCLUDING DISCUSSION

In our proposed explanation of the large-scale emission characteristics of G327 and G296 we have expanded upon an old idea that the bright flanks of emission correspond to regions where compression of the interstellar field by the advancing shock is most effective. We contend, however, that field enhancement per se is insufficient to account for the bilateral symmetry in the radio and X-ray emission. Conditions in the vicinity of the shock may be dependent upon the direction of propagation relative to the preshock field and may determine the efficiency of particle heating and the acceleration rate in the emitting plasma. The observations seem consistent with the contention of Jokipii (1987) that the energy gain of fast charged particles is a strong function of the angle between the shock direction and the ambient field. We further propose that as a remnant ages the coupling of interstellar gas behind a quasi-parallel shock may be progressively less efficient resulting in less deceleration (and a greater diameter) for older remnants along their axis of symmetry. The lack of a definite shock boundary along the axis directions could affect the shock's ability to preionize upstream neutral material and, consequently, to couple to it. That some neutral material does indeed cross the shock on the northern axis of G327 is indicated by the Balmer emission at this point.

The sudden decline in emission at $\sim 18°$ from the southern axis of G296 may represent a "critical angle" for the quasi-parallel propagation. Clearly a search for similar phenomena in other remnants would be valuable.

As seen in our maps, G296.5+10.0 and G327.6+14.6 display an unusually high degree of bilateral symmetry. The radio emission from another high-latitude evolved remnant, G93.3+6.9 (Haslam, Pauls, and Salter 1980), is also highly symmetric and unusually highly polarized. We suggest that in regions removed from the Galactic plane, there is a significantly greater probability that an SNR will expand into a large volume with an orderly magnetic field. However, even at lower latitudes, some degree of bilateral symmetry is clearly discernible in a number of shell remnants such as G46.8−0.3 (Caswell *et al.* 1975), G302.3+0.7 (Clark, Caswell, and Green 1975), and even G332.4+0.1 (Roger *et al.* 1985). Several remnants in the Magellanic Clouds also show bilateral symmetry both in their radio (Mills *et al.* 1984) and in their optical (Mathewson *et al.* 1983) emission. Remnants whose fields are oriented such that we view them almost along the ambient field direction should show mainly circular symmetry. If we imagine the angle between the field and the line of sight increasing, the first manifestation of bilateral symmetry would likely be a weakening of the shell emission at diametrically opposite portions of the shell, at the points where the shock propagation is quasi-parallel. For SNRs close to the Galactic plane, where the interstellar field may be relatively disordered, many isolated weak or missing sections of shell emission may be the result of small-scale distortions of the field producing localized regions of quasi-parallel propagation. However, since density and field irregularities may well be correlated, and both will be swept up and modified by an expanding shock front, the unraveling of various factors contributing to emission variations is unlikely to be straightforward.

Detailed studies, possibly with numerical simulations similar to those which have been used to model conditions near magnetospheric or interplanetary shocks (e.g. Quest 1985) are needed to test the proposals we have advanced to explain various aspects of the emission symmetry in G296 and G327.

We have ascribed the filamentary components of radio emission in G296 to shocked, partially cooled, and compressed clouds, still too hot to radiate significantly in the optical. However, although many older remnants have filaments which roughly coincide in the radio and optical, studies of the detailed correspondences are lacking, and it is quite possible that radio filaments often precede detectable optical emission. New optical observing techniques of high sensitivity (e.g. narrow-band CCD imaging) can be employed to help elucidate the interrelation of the various gas components of radiating sheets and filaments.

We are indebted to Professor B. Y. Mills, the late Professor A. G. Little, and J. M. Durdin for their assistance and counsel in our observing with the Molonglo synthesis telescope. The Molonglo Observatory is funded by the Australian Research Grants Committee, the University of Sydney Research Committee, and the Science Foundation for Physics within the university. We thank an anonymous referee for helpful suggestions.

REFERENCES

Bame, S. J., Asbridge, J. R., Gosling, J. T., Halbig, M., Paschmann, G., Sckopke, N., and Rosenbauer, H. 1979, *Space Sci. Rev.*, **23**, 75.
Bazer, J., and Ericson, W. B. 1959, *Ap. J.*, **129**, 758.
Bisnovatyi-Kogan, G. S., and Blinnikov, S. I. 1982, *Soviet Astr.*, **26**, 530.
Blandford, R. D., and Cowie, L. L. 1982, *Ap. J.*, **260**, 625.
Bodenheimer, P., and Woosley, S. E. 1983, *Ap. J.*, **269**, 281.
Bohlin, R. C., Savage, B. D., and Drake, J. F. 1978, *Ap. J.*, **224**, 132.
Borovsky, J. E., Pongratz, M. B., Roussel-Dupre, R. A., and Tan, Tai-Ho. 1984, *Ap. J.*, **280**, 802.
Braun, R., and Strom, R. G. 1986, *Astr. Ap.*, **164**, 193.
Caswell, J. L. 1979, *M.N.R.A.S.*, **187**, 431.
Caswell, J. L., Clark, D. H., and Crawford, D. F. 1975, *Australian J. Phys., Ap. Suppl.*, No. 37, p. 39.
Caswell, J. L., Haynes, R. F., Milne, D. K., and Wellington, K. J. 1983, *M.N.R.A.S.*, **204**, 921.
Caswell, J. L., and Lerche, L. 1979, *M.N.R.A.S.*, **187**, 201.
Celnick, W., Rohlfs, K., and Braunsfurth, E. 1979, *Astr. Ap.*, **76**, 24.
Chevalier, R. A. 1974, *Ap. J.*, **188**, 501.
Clark, D. H., Caswell, J. L., and Green, A. 1975, *Australian J. Phys., Ap. Suppl.*, No. 37, p. 1.
Colomb, F. R., Poppel, W. G. L., and Heiles, C. 1980, *Astr. Ap. Suppl.*, **40**, 47.
Cox, D. P., and Daltabuit, E. 1971, *Ap. J.*, **167**, 113.
Dickel, J. R., and Milne, D. K. 1976, *Australian J. Phys.*, **29**, 435.
Dubner, G. M., Colomb, F. R., and Giacani, E. B. 1986, *A.J.*, **91**, 343.
Ellis, R. S., and Axon, D. J. 1978, *Ap. Space Sci.*, **54**, 425.
Galas, C. M. F., Venkatesan, D., and Garmire, G. 1982, *Ap. Letters*, **22**, 103.
Gardner, F. F., and Milne, D. K. 1965, *A.J.*, **70**, 754.
Hamilton, A. J. S., Sarazin, C. L., and Szymkowiak, A. E. 1986, *Ap. J.*, **300**, 698.
Haslam, C. G. T., Pauls, T., and Salter, C. J. 1980, *Astr. Ap.*, **92**, 57.
Helfand, D. J., and Becker, R. H. 1984, *Nature*, **307**, 215.
Hesser, J. E., and van den Bergh, S. 1981, *Ap. J.*, **251**, 549.
Hollenbach, D., and McKee, C. F. 1979, *Ap. J. Suppl.*, **41**, 555.
Irvine, N. J., and Irvine, C. E. 1974, *Ap. J. (Letters)*, **192**, L111.
Jackson, P. D., and Kellman, S. A. 1974, *Ap. J.*, **190**, 53.
Jokipii, J. R. 1987, *Ap. J.*, **313**, 842.
Kellett, B. J., Branduardi-Raymont, G., Culhane, J. L., Mason, I. M., Mason, K. O., and Whitehouse, D. R. 1987, *M.N.R.A.S.*, **225**, 199.
Kerr, F. J., Bowers, P. F., Jackson, P. D., and Kerr, M. 1986, *Astr. Ap.*, **66**, 373.
Kesteven, M. J., and Caswell, J. L. 1987, *Astr. Ap.*, **183**, 118.
Kirshner, R. P., Winkler, P. F., and Chevalier, R. A. 1987, *Ap. J. (Letters)*, **315**, L135.
Kulsrud, R. M., Bernstein, I. B., Kruskal, M., Fanucci, J., and Ness, N. 1965, *Ap. J.*, **142**, 491.
Lasker, B. M. 1966, *Ap. J.*, **146**, 471.
———. 1981, *Ap. J.*, **244**, 517.
Manchester, R. N., D'Amico, N., and Tuohy, I. R. 1985, *M.N.R.A.S.*, **212**, 975.
Mathewson, D. S., and Ford, V. L. 1971, *Mem. R. A. S.*, **74**, 139.
Mathewson, D. S., Ford, V. L., Dopita, M. A., Tuohy, I. R., Long, K. S., and Helfand, D. J. 1983, *Ap. J. Suppl.*, **51**, 345.
Mathis, J. S. 1986, *Ap. J.*, **301**, 423.
Matsui, Y., Long, K. S., and Tuohy, I. R. 1988, in *IAU Colloquium 101, Supernova Remnants and the Interstellar Medium*, ed. R. S. Roger and T. L. Landecker (Cambridge: Cambridge University Press), p. 157.
McKee, C. F., and Cowie, L. L. 1975, *Ap. J.*, **195**, 715.
McKee, C. F., and Ostriker, J. P. 1977, *Ap. J.*, **218**, 148.
McKee, C. F., van Buren, D., and Lazareff, B. 1984, *Ap. J. (Letters)*, **278**, L115.
Mills, B. Y. 1981, *Proc. Astr. Soc. Australia*, **4**, 156.
Mills, B. Y., Turtle, A. J., Little, A. G., and Durdin, J. M. 1984, *Australian J. Phys.*, **37**, 321.
Milne, D. K. 1971, *Australian J. Phys.*, **24**, 757.
———. 1979, *Australian J. Phys.*, **32**, 83.
Milne, D. K., and Dickel, J. R. 1975, *Australian J. Phys.*, **28**, 209.
Pye, J. P., Pounds, K. A., Rolf, D. P., Seward, F. D., Smith, A., and Willingale, R. 1981, *M.N.R.A.S.*, **194**, 569.
Quest, K. B. 1985, *Phys. Rev. Letters*, **54**, 1872.
Reynolds, S. P., and Chevalier, R. A. 1981, *Ap. J.*, **245**, 912.
Reynolds, S. P., and Gilmore, D. M. 1986, *A.J.*, **92**, 1138.
Roger, R. S., Milne, D. K., Kesteven, M. J., Haynes, R. F., and Wellington, K. J. 1985, *Nature*, **316**, 44.
Roger, R. S., Milne, D. K., Wellington, K. J., Haynes, R. F., and Kesteven, M. J. 1984, *Proc. Astr. Soc. Australia*, **5**, 560.
Ruiz, M. T. 1983, *A.J.*, **88**, 1210.
Shaver, P. A. 1969, *Observatory*, **89**, 227.
———. 1982, *Astr. Ap.*, **105**, 306.
Shull, J. M., and McKee, C. F. 1979, *Ap. J.*, **227**, 131.
Shull, P., Dyson, J. E., Kahn, F. D., and West, K. A. 1985, *M.N.R.A.S.*, **212**, 799.
Stephenson, F. R., Clark, D. H., and Crawford, D. F. 1977, *M.N.R.A.S.*, **180**, 567.
Thomson, R. C., and Nelson, A. H. 1980, *M.N.R.A.S.*, **191**, 863.
Tuohy, I. R., Mason, K. O., Clark, D. H., Cordóva, F. A., Charles, P. A., Walter, F. M., and Garmire, G. P. 1979, *Ap. J. (Letters)*, **230**, L27.
van den Bergh, S. 1976, *Ap. J. (Letters)*, **208**, L17.
van der Laan, H. 1962, *M.N.R.A.S.*, **124**, 179.
Vartanian, M. H., Lum, K. S. K., and Ku, W. H-M. 1985, *Ap. J. (Letters)*, **288**, L5.
Whiteoak, J. B., and Gardner, F. F. 1968, *Ap. J.*, **154**, 807.
Wu, C-C., Leventhal, M., Sarazin, C. L., and Gull, T. R. 1983, *Ap. J. (Letters)*, **269**, L5.

R. F. Haynes, M. J. Kesteven, D. K. Milne, and K. J. Wellington: Division of Radiophysics, CSIRO, P.O. Box 76, Epping, N.S.W., Australia 2121

R. S. Roger: Dominion Radio Astrophysical Observatory, Herzberg Institute of Astrophysics, P.O. Box 248, Penticton, B.C. V2A 6K3, Canada